Steady oscillations in aggregation-fragmentation processes

N. V. Brilliantov,[1,2,*] W. Otieno,[1] S. A. Matveev,[2] A. P. Smirnov,[3,4] E. E. Tyrtyshnikov,[3,4] and P. L. Krapivsky[5]

[1]*Department of Mathematics, University of Leicester, Leicester LE1 7RH, United Kingdom*

[2]*Skolkovo Institute of Science and Technology, Moscow, Russia*

[3]*Faculty of Computational Mathematics and Cybernetics, Lomonosov MSU, Moscow, Russia*

[4]*Institute of Numerical Mathematics RAS, Moscow, Russia*

[5]*Department of Physics, Boston University, Boston, Massachusetts 02215, USA*

(Received 2 March 2018; revised manuscript received 14 May 2018; published 11 July 2018)

We report surprising steady oscillations in aggregation-fragmentation processes. Oscillating solutions are observed for the class of aggregation kernels $K_{i,j} = i^\nu j^\mu + j^\nu i^\mu$ homogeneous in masses i and j of merging clusters and fragmentation kernels, $F_{ij} = \lambda K_{ij}$, with parameter λ quantifying the intensity of the disruptive impacts. We assume a complete decomposition (shattering) of colliding partners into monomers. We show that an assumption of a steady-state distribution of cluster sizes, compatible with governing equations, yields a power law with an exponential cutoff. This prediction agrees with simulation results when $\theta \equiv \nu - \mu < 1$. For $\theta = \nu - \mu > 1$, however, the densities exhibit an oscillatory behavior. While these oscillations decay for not very small λ, they become steady if θ is close to 2 and λ is very small. Simulation results lead to a conjecture that for $\theta < 1$ the system has a stable fixed point, corresponding to the steady-state density distribution, while for any $\theta > 1$ there exists a critical value λ_c, such that for $\lambda < \lambda_c$, the system has an attracting limit cycle. This is rather striking for a closed system of Smoluchowski-like equations, lacking any sinks and sources of mass.

DOI: 10.1103/PhysRevE.98.012109

I. INTRODUCTION

Numerous phenomena in nature involve dual processes of aggregation and fragmentation [1,2]. These processes take place on vastly different length and time scales. A reversible polymerization in solutions and coagulation of colloidal particles are the classical examples of such processes occurring on the molecular scales; another peculiar example is aggregation of prions causing the Alzheimer-like diseases [3]. On the larger scales—in atmospheric processes, small airborne particles coalesce into smog droplets [4]. Aggregation is also common in systems of living organisms, from colonies of viruses [5] to schools of fish [6]. Aggregation and fragmentation processes occur in networks of different nature, including economic networks [7] and internet communities [1,8]; here forums of users nucleate, merge, and split. In turbulent cascades in a fluid flow [9] vortices may merge forming larger ones or decomposing into smaller vortices. The distribution of particles size in planetary rings is also determined by a steady balance achieved between two opposite processes, viz. aggregation and breakage of the particles in the rings [10–14].

A. Aggregation

The aggregation takes place when two clusters, comprised respectively of i and j monomers, merge upon collision thereby creating a cluster of $i + j$ monomers (see Fig. 1); symbolically this process may be written as

$$[i] + [j] \longrightarrow K_{ij}[i + j],$$

where K_{ij} is the merging rate. Let n_k be the concentration of clusters of size k, i.e., clusters composed of k monomers. The rate of change of n_k is determined by Smoluchowski equations [1,2]

$$\frac{dn_k}{dt} = \frac{1}{2}\sum_{i+j=k} K_{i,j} n_i n_j - n_k \sum_{i=1}^{\infty} K_{i,k} n_i. \tag{1}$$

The first term on the right-hand side accounts for the formation rate of k-mers from clusters of size i and j, the second term describes the loss of k-mers due to aggregation of these clusters with all other clusters; the factor $1/2$ in the first term prevents from double counting of the same process ($i + j \to k$ and $j + i \to k$).

B. Aggregation with fragmentation

Generally aggregates can suffer both spontaneous and collision fragmentation [1–3,10,11,13]. In the former case a cluster breaks into smaller pieces without interactions with other aggregates [1–3], in the latter one the fragmentation is caused by an energetic impact between two clusters [10,11,13]. Different collision fragmentation models have been studied [10,11,13]; here we will consider a simple one of complete shattering of two colliding partners into monomers. Symbolically this process (see Fig. 1) may be written as

$$[i] + [j] \xrightarrow{F_{ij}} \underbrace{[1] + [1] + \ldots [1]}_{i+j},$$

where F_{ij} quantifies the shattering rate. Models with shattering exhibit interesting behaviors including dynamical phase transitions [15]. It has been shown [10] that more general fragmentation models with a large number of fragments yield

*Corresponding author: nb144@leicester.ac.uk

 ©2018 American Physical Society

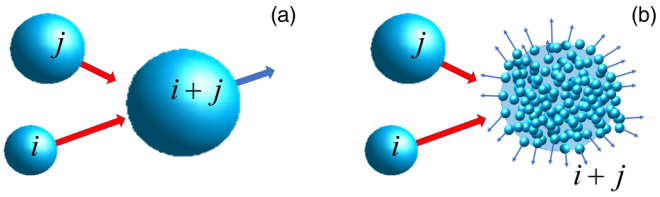

FIG. 1. (a) A merging event. (b) A collision of clusters of size i and j leading to decomposition into $i + j$ monomers.

qualitatively similar size distribution provided the small-size debris strongly dominates over the large size ones [10]. As in Ref. [10], we assume that the fragmentation and aggregation kernels are proportional,

$$F_{ij} = \lambda K_{ij}, \tag{2}$$

as has been justified for processes in planetary rings [10]. The parameter λ in Eq. (2) characterizes the relative frequency of aggregative and shattering impacts.

Adding the fragmentation kinetics with kernel (2) into kinetic equations (1) we arrive at a separate equation

$$\frac{dn_1}{dt} = -n_1 \sum_{i=1}^{\infty} K_{1,i} n_i + \frac{\lambda}{2} \sum_{i=2}^{\infty} \sum_{j=2}^{\infty} (i+j) K_{i,j} n_i n_j + \lambda n_1 \sum_{j=2}^{\infty} j K_{1,j} n_j \tag{3}$$

for the concentration of monomers and a set of generic equations

$$\frac{dn_k}{dt} = \frac{1}{2} \sum_{i=1}^{k-1} K_{i,k-i} n_i n_{k-i} - (1+\lambda) n_k \sum_{i=1}^{\infty} K_{k,i} n_i \tag{4}$$

for $k \geqslant 2$. The second term on the right-hand side of Eq. (3) accounts for the gain of monomers occurring in shattering collisions between clusters, and the third term describes the gain of monomers in the shattering impacts between monomers and clusters. Equation (4) differs from (1) by an extra loss term (proportional to λ) accounting for shattering.

Equations (3) and (4) describe spatially homogeneous systems. The kernels $K_{i,j}$ may be obtained from the microscopic analysis of the aggregation and fragmentation processes (see, e.g., [10,13,16] and the Appendix). In applications, $K_{i,j}$ are usually homogeneous functions of the masses i and j of merging clusters. Here we will investigate the kernels

$$K_{i,j} = i^{\nu} j^{\mu} + i^{\mu} j^{\nu} \tag{5}$$

which are rather popular [1,2] and have been used for similar aggregating-shattering systems in Ref. [17] where a source of monomers and sink of large aggregates was present. A stationary distribution satisfying Eqs. (3) and (4) with the kernel (5) has been also addressed in [18].

In the following, we shall often use the sum and the difference of the exponents μ and ν,

$$\beta = \nu + \mu, \quad \theta = \nu - \mu. \tag{6}$$

(Without loss of generality, we choose $\nu \geqslant \mu$.) The exponent β is the well-known homogeneity exponent [1,2]. The exponent θ plays an important role in the following; it has been called a nonlocality exponent in [17,18].

We always limit ourselves to the nongelling case $\beta < 1$. The restrictions $\nu \leqslant 1$ and $\mu \leqslant 1$ are needed to avoid instantaneous gelation (see, e.g., [19–23]). The exponent θ can exceed 1, and never-ending oscillations are actually observed in a "nonlocal" regime $\theta > 1$.

In the special case of $\nu = -\mu = a$, the kernel reads

$$K_{i,j} = i^a j^{-a} + j^a i^{-a} \tag{7}$$

with $0 \leqslant a \leqslant 1$. This kernel is known as a generalized Brownian kernel [24]. In what follows we will analyze both (5) and (7), often starting with the latter which is more tractable. The restriction $a \leqslant 1$ is needed to avoid instantaneous gelation (aggregation equations with $a > 1$ are ill-defined [19–23,25]). The solutions of the aggregation-fragmentation equations should also satisfy the natural physical requirement $n_k(t) \geqslant 0$, and mass conservation:

$$M = \sum_{k=1}^{\infty} k n_k(t) \equiv \text{const}. \tag{8}$$

Analytical time-dependent solutions to Eqs. (3) and (4), have been obtained only for the simplest case of a constant kernel [10]. The steady-state solutions have been found for several other models, such as an irreversible aggregation model with a monomer source [26], an aggregation-fragmentation model with kernels $K_{i,j} = (ij)^{\mu}$ and $F_{i,j} = \lambda K_{i,j}$ [10], and for an open aggregation-fragmentation system with a source of monomers and sink of large clusters [17] for the kernels of the form (5) and for closed systems in [18]. An *open* aggregating system with the same coagulation kernel (5), driven by input of monomers along with the removal of large clusters, has been studied in [27]. Steady oscillations were numerically found in this system with a finite number of aggregate species [27]. For a closed system comprised of monomers, dimers, trimers, and exited monomers, stable oscillations have been also reported [28]. Similarly, steady chemical oscillations may occur in a dimerization model (see, e.g., [29]).

In the present study we consider *closed* systems undergoing aggregation and fragmentation processes, with the kinetic rates given by Eqs. (5) and (2), that lack any source or sink of monomers and clusters. Naively, one expects that such closed systems with two opposite processes will relax to a steady state where a balance between aggregation and shattering is established. This scenario is indeed realized for $\theta < 1$, or $a < 1/2$ in the case of the kernels (7). Unexpectedly, for $\theta \to 2$ (or $a \to 1$) and small values of λ we observe never-ending oscillations of the concentrations. This effect has been found numerically for the one-parameter family of kernels (7) and reported in our recent study [30]. Here we present a more detailed analysis of the aggregating and shattering systems, both numerical and theoretical, and we investigate a more general two-parameter family of kernels (5). We also provide a qualitative theory of the stable oscillations which sheds some light on the mechanism of this surprising phenomenon.

In what follows, we will concentrate on systems with time-independent coefficients K_{ij} and λ, and conserved total mass (total number of elementary units). This is a generic model that describes systems of very different nature. The elements comprising a system range from grains or molecules

to living organisms or economic agents. The interaction forces, that determine the kinetic rates, may be of very different nature as well. These may range from true molecular or mechanical forces to fictious "social forces" [31], based on informational exchange. Therefore, strictly speaking, the term "closed" here literally means a lack of sinks and sources of system elements. At the same time, the exchange of energy, chemicals, nutrients, and information is implied. This is needed to sustain elements of a system and keep the rate coefficients steady. On the level of social agents or a living organism this implies an interaction with the surrounding social or natural environment. On the level of molecular or macroscopic particles the interaction with a thermostat, or the presence of some other source of energy, is assumed. For instance, in aggregation-fragmentation processes in polymer or colloidal solutions, there exists energy exchange with the solvent. This maintains constant temperature, although energy is released in aggregation processes and consumed in fragmentation processes. Similarly the surrounding molecular gas plays a role of thermostat in atmospheric processes [32] and for dust clouds [33,34]. Another important mechanism of energy supply is viscous heating, which arises in planetary rings [14]. In this case the orbital motion of rings' particles yields a sheared flow of viscous granular fluid, which generates heat [14]. The energy supply keeps the kinetic energy of aggregates steady, and the rate coefficients constant.

Systems with true molecular or mechanical forces between elements is an important subclass of systems with aggregation and fragmentation. As it follows from the discussion above, such systems, with constant rate coefficients, are not thermodynamically closed. (Note that the notion "thermodynamics" is meaningful only for these systems.) Hence an interesting question arises—whether persistent concentration oscillations exist in *thermodynamically* closed systems? We perform a microscopic analysis, which resulted in a positive answer: Never-ending oscillations do emerge in thermodynamically closed systems, although the oscillation period permanently increases.

The rest of the paper is organized as follows. In the next section, Sec. II, we present simulation results obtained with the use of fast solvers of Smoluchowski-type equations. In Sec. III we discuss steady-state distributions using the methods outlined in Ref. [30] and applied to Brownian kernels $\mu = -\nu = a$. We also present a qualitative theory explaining the mechanism leading to never-ending oscillations and analyze oscillation behavior in thermodynamically closed systems. In Sec. IV we summarize our findings.

II. NUMERICAL RESULTS

Kinetic equations (3) and (4) form a set of infinitely many nonlinear coupled ordinary differential equations (ODEs), which is a severe numerical challenge. For standard Smoluchowski equations, that is, when fragmentation is absent, the average size of aggregates grows indefinitely imposing a time limit to model these processes. Fragmentation precludes the formation of very large clusters (in most cases and certainly in our case when fragmentation and aggregation kernels are proportional). This allows us to model the aggregating-and-shattering systems with a finite number of equations $N_{\rm eq}$, which is dictated by the requested accuracy. In Ref. [30] we present estimates that relate the number of equations and the simulation accuracy; in practice we use such number of equations that a further increase of $N_{\rm eq}$ does not impact the results for the concentrations $n_k(t)$ within the numerical precision.

The structure of the kinetic kernels (7) allows us to apply highly efficient numerical methods, in particular, the fast and accurate method of time integration of Smoluchowski-type equations [35–39]. The efficiency and accuracy of this approach in solving the aggregating-and-shattering equations has been demonstrated in Ref. [30], where the numerical results have been compared with the available analytical solutions [10].

A. Steady-state size distribution

Solving numerically Eqs. (3) and (4) with kernel (7) for $a < 1/2$, we observe that the concentrations relax monotonically to a steady state; see Fig. 2. In Fig. 2 we also compare the numerical results with the analytical solution for the steady-state distribution n_k, discussed below. The numerical and analytical solutions agree fairly well.

Similar behavior is observed for the general kernel (5). When $\theta = \mu - \nu < 1$, the concentrations relax monotonically to a steady state, and the final distribution agrees with the one predicted theoretically; see Fig. 3. The steady-state size distribution may be interpreted as a stable fixed point in the language of dynamical systems [40].

B. Oscillating solutions

1. Brownian kernels ($\nu = -\mu = a$)

For $a \geqslant 1/2$ a relaxation to a steady-state distribution occurs through oscillations, provided the parameter λ, quantifying the shattering intensity, is relatively small. This is illustrated in Fig. 4, where the time dependence of the total number of aggregates, $N(t) = \sum_{k\geqslant 1} n_k(t)$, is shown; the figure also demonstrates that the oscillations are more pronounced and persist for longer time as a increases, while λ decreases.

We found the oscillations independently of initial conditions; here we use the monodisperse initial conditions, $n_k(0) = M\delta_{1,k}$, and stepwise initial conditions

$$n_k(t=0) = \begin{cases} 0.1 & k = 1,2,\ldots 10 \\ 0 & k > 10 \end{cases}, \tag{9}$$

with the same total mass $M = 5.5$. Unless explicitly stated, the reported results refer to the initial conditions (9). For $a \to 1$ and relatively small λ we observe stable, seemingly never-ending oscillations, see Fig. 5, where the temporal behaviors of the total density $N(t)$ and the second moment $M_2(t) = \sum_{k\geqslant 1} k^2 n_k(t)$ are depicted.

Making the time averaging of the densities over the oscillation period, one obtains the distribution of the averaged quantities $\langle n_k\rangle_{\rm osc}$, which has a form of the power law with a cutoff at $k \sim k_0$; see Fig. 6:

$$\langle n_k\rangle_{\rm osc} \sim k^{-\alpha}, \qquad \alpha \simeq 5/4, \quad k < k_0. \tag{10}$$

2. General kernels (5)

We observed oscillations for the general kernel (5) when $\theta = \nu - \mu > 1$ (which corresponds to $a > 1/2$ of the Brow-

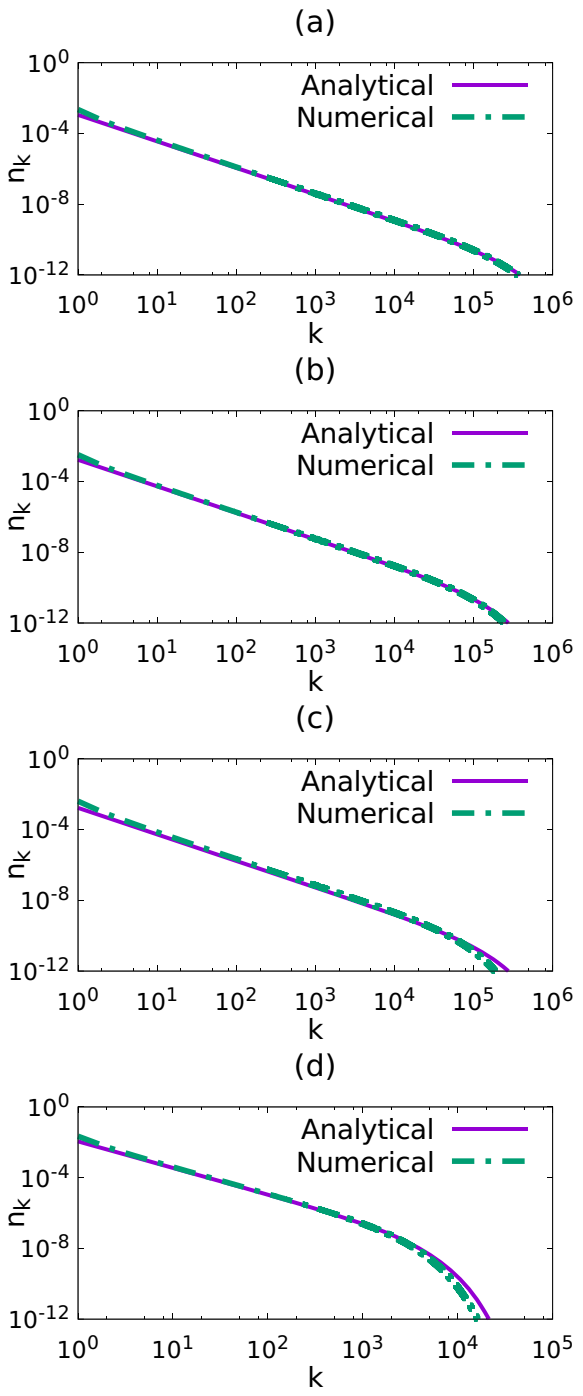

FIG. 2. Steady-state distributions obtained numerically by solving Eqs. (3) and (4) for the Brownian kernel (7). Analytical results, Eq. (29), are also shown. The model parameters are set as (a) $a = 0.05$, $\lambda = 0.002$, (b) $a = 0.05$, $\lambda = 0.003$, (c) $a = 0.1$, $\lambda = 0.003$, (d) $a = 0.1$, $\lambda = 0.005$.

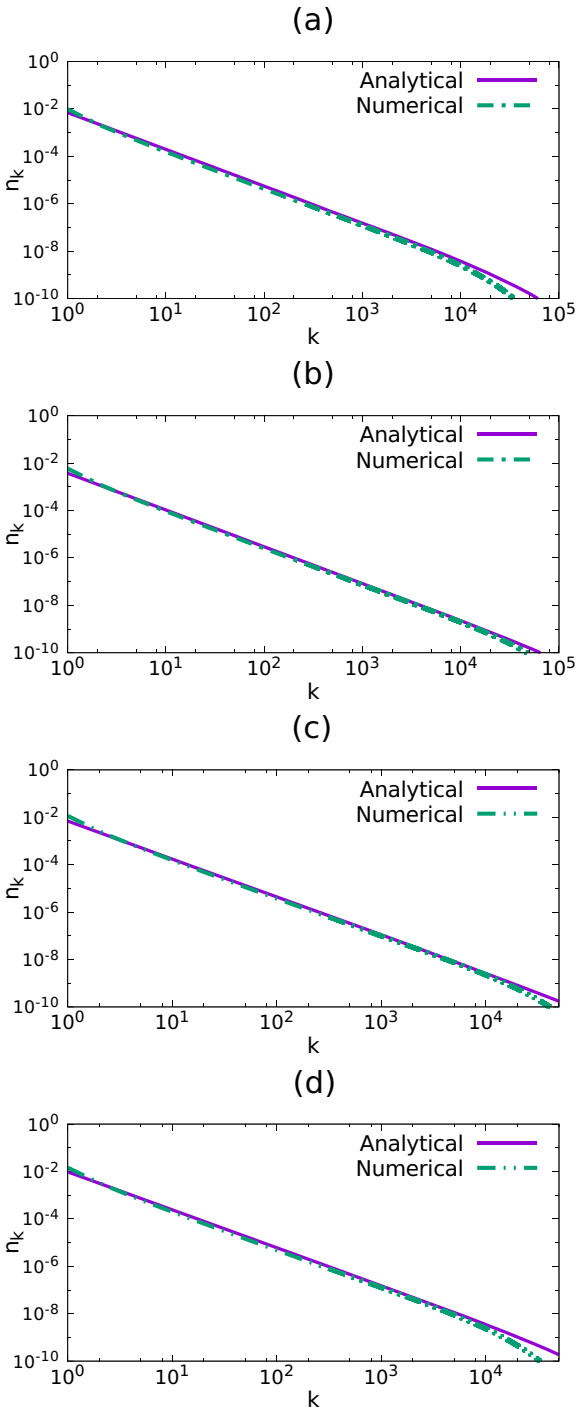

FIG. 3. Steady-state distributions obtained numerically by solving Eqs. (3) and (4) for kernels (5) with $\theta = \nu - \mu < 1$. Analytical results, Eq. (26), are also shown. The model parameters are set as (a) $\nu = 0.2$, $\mu = -0.1$, $\lambda = 0.004$, (b) $\nu = 0.2$, $\mu = -0.1$, $\lambda = 0.002$, (c) $\nu = 0.3$, $\mu = -0.1$, $\lambda = 0.002$, (d) $\nu = 0.3$, $\mu = -0.1$, $\lambda = 0.003$.

nian kernel). However, if θ is not close to $\theta = 2$, the system relaxes to a steady distribution through the damped oscillations, even for rather small λ; see Fig. 7.

When $\theta \to 2$ (which corresponds to $a \to 1$), steady oscillations emerge for small λ. The larger the exponent θ, the larger the shattering rate λ where steady oscillations emerge; see Fig. 8.

Our simulations imply the existence of a critical value $\lambda_c(\theta)$ such that for $\lambda < \lambda_c(\theta)$ in the long time limit the system

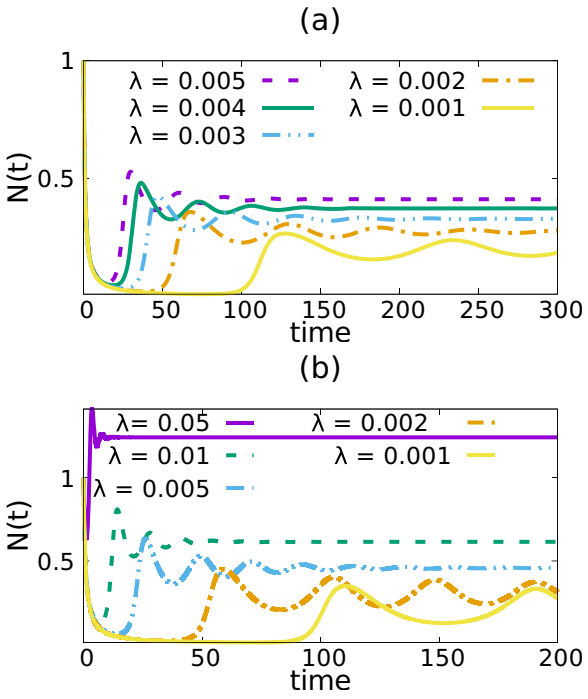

FIG. 4. Time dependence of the total density for $a = 0.7$ (a) and $a = 0.75$ (b) and different λ. The system relaxes to a steady state through damped oscillations which are more pronounced for larger a and smaller λ.

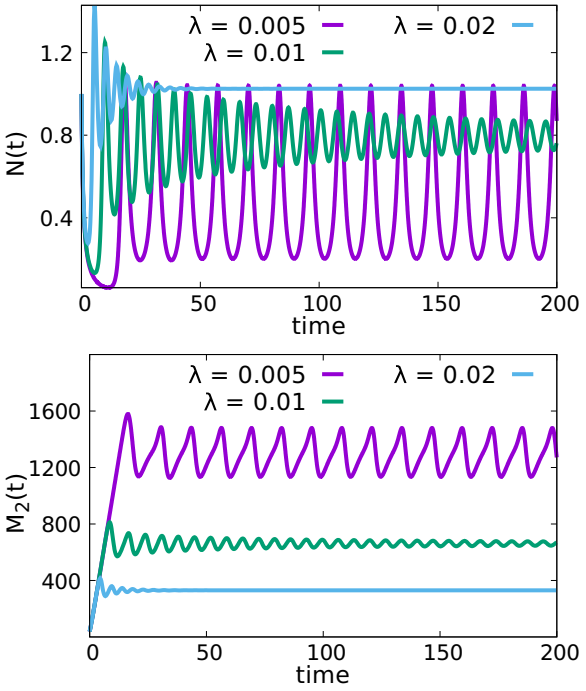

FIG. 5. Time dependence of the clusters density $N(t)$ (top) and the second moment $M_2(t) = \sum_{k\geqslant 1} k^2 n_k(t)$ (bottom), for the kernel (7) with $a = 0.9$ and different λ. Seemingly never-ending oscillations are observed for $\lambda = 0.005$.

approaches a limit cycle, viz. concentrations exhibit never-ending oscillations. This has been checked for the Brownian kernel and for the general kernel (5). Although for $a < 0.9$ we have observed only damped oscillations, we believe that never-ending oscillations would emerge for all $a > 1/2$ and sufficiently small λ. This is seemingly true for the general case: The steady oscillations would be observed for any $\theta > 1$ if λ is small enough. We cannot prove this numerically due to an unaccessible number of equations needed to simulate the systems with such small λ. For instance, to simulate the system with $a = 0.9$ and $\lambda = 0.005$ depicted in Fig. 5, more than 250 000 equations have been used. Our estimates (discussed in Ref. [30]) indicate that the number of equations $N_{\rm eq}$ needed to guarantee a requested accuracy rapidly grows with the decreasing λ. To simulate a system with $\lambda < \lambda_c$ for $a < 0.9$ one needs more than a million equations which is too large for practical implementation. Nevertheless, based on our results, we formulate the following.

Conjecture. (i) When $\theta = \mu - \nu < 1$, the system has a single stable fixed point for all values of λ; the steady-state distribution of cluster sizes n_k corresponds to this stable point. (ii) When $\theta > 1$, there exists a critical λ_c, such that for $\lambda \geqslant \lambda_c$ the system possesses a stable fixed point with the according distribution n_k. This may be a stable focus for some values of λ manifesting in damped oscillations. (iii) When $\theta > 1$ and $\lambda < \lambda_c$, the system possesses a stable limit cycle.

As it follows from our numerical results, the critical shattering λ_c strongly depends on the exponent θ; its dependence on the other exponent $\beta = \mu + \nu$ seems to be weak (if any), but is still to be studied.

III. THEORETICAL ANALYSIS

To explain theoretically the observed behavior of the aggregation-and-shattering systems we analyze separately the systems that attain a steady-state distribution and those that demonstrate never-ending oscillations. For the former case we apply the asymptotic analysis, while in the latter situation we analyze oscillations qualitatively.

A. Asymptotic analysis of a steady-state cluster size distribution

In Ref. [30] we gave a condensed account of the derivation of the steady-state distribution; here we present a more detailed derivation.

When the system reaches a steady state, differential equations (3) and (4) become algebraic equations,

$$n_1 \sum_{i=1}^{\infty} K_{1,i} n_i - \frac{\lambda}{2} \sum_{i=2}^{\infty} \sum_{j=2}^{\infty} (i+j) K_{i,j} n_i n_j$$

$$- \lambda n_1 \sum_{j=2}^{\infty} j K_{1,j} n_j = 0,$$

$$\frac{1}{2} \sum_{i=1}^{k-1} K_{i,k-i} n_i n_{k-i} - (1+\lambda) n_k \sum_{i=1}^{\infty} K_{k,i} n_i = 0, \quad k \geqslant 2. \quad (11)$$

To analyze these equations we introduce the generating functions

$$\mathcal{C}_\gamma(z) = \sum_{k=1}^{\infty} k^\gamma n_k z^k \quad (12)$$

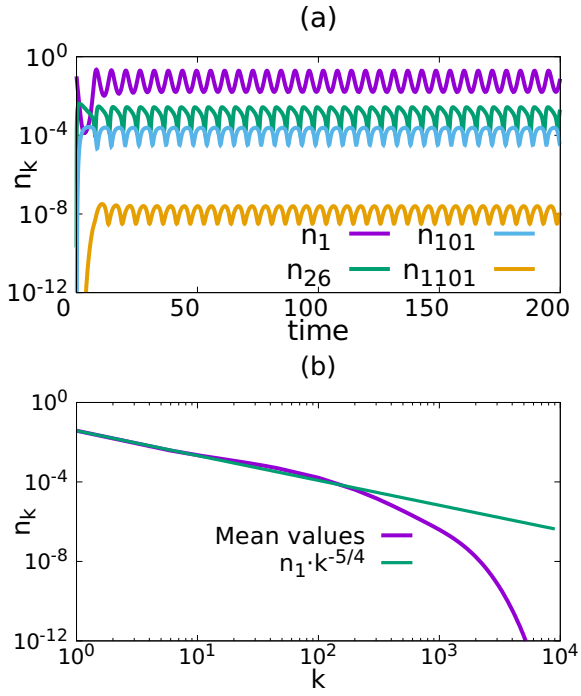

FIG. 6. Top: Stable oscillations of n_k for $a = 1.0$, $\lambda = 0.01$. Bottom: The concentration distribution after averaging over the oscillation period for $a = 0.95$, $\lambda = 0.005$. The averaged concentrations follow a power-law distribution with exponent close to $5/4$ for not too large masses.

and the moments

$$M_\gamma = \sum_{k=1}^{\infty} k^\gamma n_k.$$

Multiplying (11) by z^k and summing over all $k \geqslant 1$ we arrive at

$$\mathcal{C}_\mu(z)\mathcal{C}_\nu(z) + (1+\lambda)zn_1(M_\mu + M_\nu) - (1+\lambda)[M_\mu \mathcal{C}_\nu(z) + M_\nu \mathcal{C}_\mu(z)] = 0. \quad (13)$$

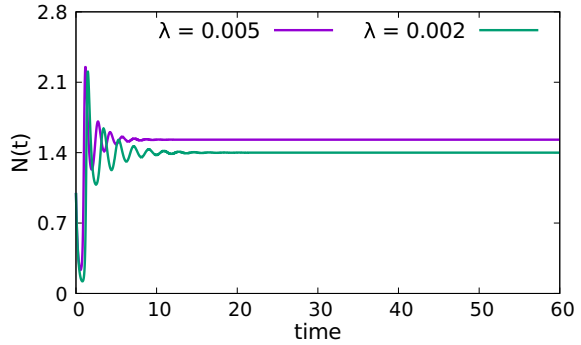

FIG. 7. The exponent $\theta = \nu - \mu = 1.2 > 1$ and $\nu = 1$, $\mu = -0.2$ is in a regime where never-ending oscillations are conjecturally possible for very small λ, but in the shown examples λ is not small enough and the cluster size distribution relaxes to a steady state through the damped oscillations (which are more pronounced for smaller λ).

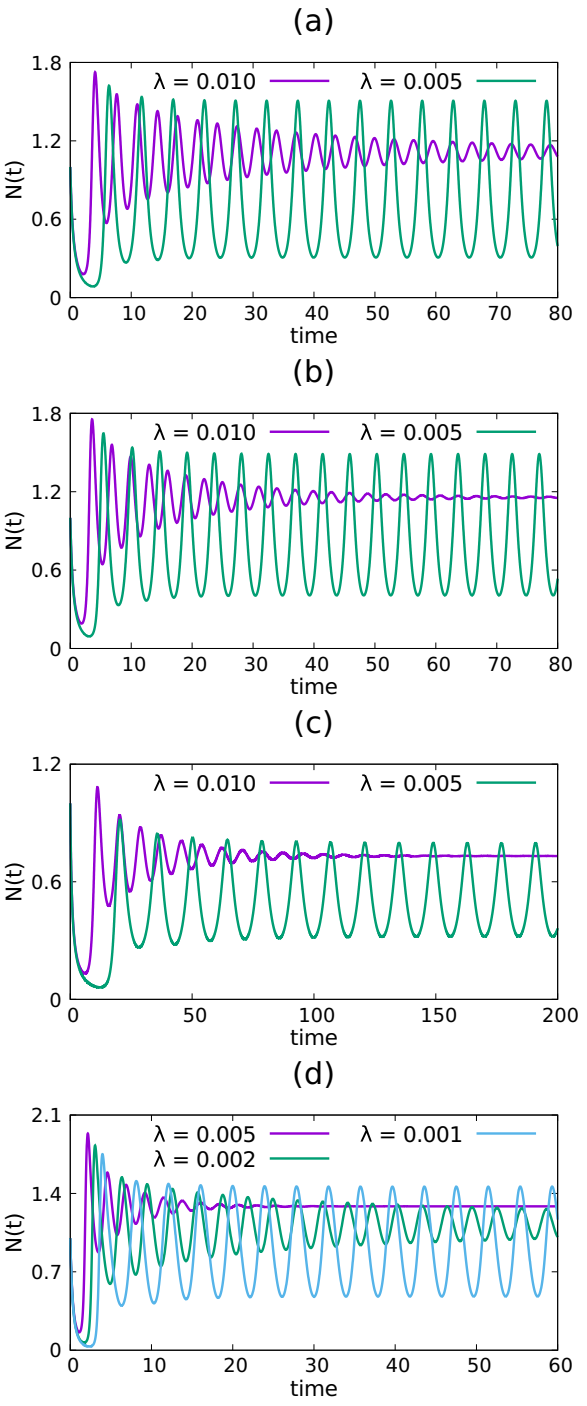

FIG. 8. Oscillating behaviors when $\theta > 1$. Never-ending oscillations emerge for rather small values of λ; overall, the larger the exponent θ, the larger the critical $\lambda_c(\theta)$ separating never-ending from damped oscillations. The model parameters are set as (a) $\nu = 1$, $\mu = -0.75$, (b) $\nu = 1$, $\mu = -0.7$, (c) $\nu = 0.85$, $\mu = -0.85$, (d) $\nu = 1$, $\mu = -0.4$.

Using $\mathcal{C}_\gamma(1) = M_\gamma$ and specializing (13) to $z = 1$ we obtain

$$M_\mu M_\nu = \frac{1+\lambda}{1+2\lambda} n_1 (M_\mu + M_\nu). \quad (14)$$

To analyze n_k for $k \gg 1$ we will use the above equations and exploit standard methods of asymptotic analysis to extract

the behavior of the generation functions $\mathcal{C}_\gamma(z)$. We consider separately kernels with $\theta < 1$ and $\theta > 1$.

1. Kernels with θ < 1 (a < 1/2).

It is known [10] that for $\mu = \nu = 0$, the tail of the steady-state distribution reads $n_k \simeq \lambda\pi^{-1/2}k^{-3/2}e^{-\lambda^2 k}$. Let us assume that for $k \gg 1$ our steady-state distribution has a similar form:

$$n_k \simeq Ck^{-\tau}e^{-\omega k} \quad \text{for} \quad k \gg 1 \tag{15}$$

with yet unknown τ, ω, and C. Equation (15) implies

$$\mathcal{C}_\gamma(z) \simeq \sum_{k=1}^{\infty} Ck^{\gamma-\tau}(z/z_0)^k = \sum_{k=1}^{\infty} Ck^{\gamma-\tau}(z')^k, \tag{16}$$

where $z_0 = e^\omega$ and $z' = z/z_0$. Obviously, $\mathcal{C}_\gamma(z')$ diverges for $z' > 1$ and converges for $z' < 1$ for all γ and τ. We assume that $\mathcal{C}_\gamma(z' = 1)$ exists, that is, $\sum_{k\geqslant 1} k^{\gamma-\tau}$ converges.

The tail of n_k is reflected in the behavior of $\mathcal{C}_\gamma(z')$ when $z' \to 1 - 0$. Suppose $\sum_{k\geqslant 1} k^{\gamma-\tau+1}$ diverges. Still, $\sum_{k\geqslant 1} k^{\gamma-\tau+1}(z')^k$ converges for $z' < 1$. The closer z' is to 1, the larger the size of the clusters k that make the main contribution to $\mathcal{C}_\gamma(z')$. Hence the dependence of $\mathcal{C}_\gamma(z')$ on z' for $z' \to 1$ characterizes the dependence of n_k on k for $k \gg 1$. To quantify this relation we differentiate $\mathcal{C}_\gamma(z)$ with respect to z:

$$\begin{aligned}
\frac{d\mathcal{C}_\gamma}{dz} &\simeq C\, z_0^{-1} \sum_{k=1}^{\infty} k^{\gamma-\tau+1}(z')^{k-1} \\
&\simeq C\, z_0^{-1} \int_0^{\infty} dk\, k^{\gamma-\tau+1} e^{k\log z'} \\
&\simeq C\, z_0^{-1} \int_0^{\infty} dk\, k^{\gamma-\tau+1} e^{-k(1-z')} \\
&= C\, z_0^{-1}\Gamma(\gamma-\tau+2)(1-z')^{\tau-\gamma-2},
\end{aligned}$$

where $\Gamma(x)$ is the gamma function and we use $z' \to 1 - 0$. Integrating with respect to z we obtain

$$\mathcal{C}_\gamma(z) = \mathcal{C}_\gamma(z_0) + C\Gamma(1+\gamma-\tau)(1-z')^{\tau-\gamma-1}. \tag{17}$$

Substituting $\mathcal{C}_\gamma(z)$ with $\gamma = \nu$ and $\gamma = \mu$ into Eq. (13) we obtain terms with different powers of $(1 - z')$. To satisfy this equation we equate to zero all these terms separately. The zero-order terms yield

$$\begin{aligned}
&\mathcal{C}_\nu(z_0)\mathcal{C}_\mu(z_0) - (1+\lambda)[M_\nu\mathcal{C}_\mu(z_0) + M_\mu\mathcal{C}_\nu(z_0)] \\
&\quad + (1+\lambda)z_0 n_1(M_\nu + M_\mu) = 0.
\end{aligned} \tag{18}$$

The terms of the order $(1 - z')^{\tau+\gamma-1}$ with $\gamma = \nu$ and $\gamma = \mu$ imply

$$\mathcal{C}_\mu(z_0)C\Gamma(1+\nu-\tau) - (1+\lambda)M_\mu C\Gamma(1+\nu-\tau) = 0, \tag{19}$$

$$\mathcal{C}_\nu(z_0)C\Gamma(1+\mu-\tau) - (1+\lambda)M_\nu C\Gamma(1+\mu-\tau) = 0. \tag{20}$$

Finally, the rest of the terms should satisfy

$$\begin{aligned}
&C^2\Gamma(1+\nu-\tau)\Gamma(1+\mu-\tau)(1-z')^{2\tau-\nu-\mu-2} \\
&\quad - (1+\lambda)z_0 n_1(M_\nu + M_\mu)(1-z') = 0
\end{aligned} \tag{21}$$

from which $2\tau - \nu - \mu - 2 = 1$, or

$$\tau = \frac{3+\beta}{2}, \tag{22}$$

where $\beta = \nu + \mu$. Now we substitute

$$\mathcal{C}_\gamma(z_0) = (1+\lambda)M_\gamma, \tag{23}$$

which follows from (19) and (20) into (18) to obtain

$$M_\nu M_\mu = \frac{z_0}{1+\lambda} n_1(M_\nu + M_\mu). \tag{24}$$

From Eqs. (24) and (14) we get

$$z_0 = e^\omega = \frac{(1+\lambda)^2}{(1+2\lambda)}. \tag{25}$$

We have $\omega \simeq \lambda^2 - 2\lambda^3 + \cdots \simeq \lambda^2$ for small λ leading to

$$n_k \simeq \frac{C}{k^{(3+\beta)/2}} e^{-\lambda^2 k} \quad \text{for} \quad k \gg 1. \tag{26}$$

To estimate the constant C we utilize the distribution (26) together with mass conservation to yield

$$\begin{aligned}
M = \sum_{k=1}^{\infty} kn_k &\approx \int_1^{\infty} dk\, \frac{C}{k^{(1+\beta)/2}} e^{-\lambda^2 k} \\
&\simeq C\lambda^{\beta-1}\Gamma\left(\frac{1-\beta}{2}\right)
\end{aligned} \tag{27}$$

resulting in

$$C \simeq \frac{M\lambda^{1-\beta}}{\Gamma[(1-\beta)/2]} \sim \lambda^{1-\beta}M. \tag{28}$$

In the nongelling $\beta < 1$ region, the major contribution to the integral in (27) comes from $k \gg 1$, so the usage of (26) is justified. For the Brownian kernel $\nu = -\mu = a$ and $\beta = 0$, so the amplitude is $C \simeq \lambda M/\sqrt{\pi}$ and

$$n_k \simeq \frac{\lambda M}{\sqrt{\pi}k^{3/2}} e^{-\lambda^2 k} \quad \text{for} \quad k \gg 1. \tag{29}$$

2. Kernels with θ > 1 (a > 1/2)

Applying the same analysis for $\theta \geqslant 1$ (or $a \geqslant 1/2$), one arrives at Eqs. (18)–(21), which however do not lead to consistent results. Indeed, from Eq. (21) it follows that $\tau = (3 + \nu + \mu)/2$, then substituting $\tau = (3 + \nu + \mu)/2$ into Eq. (16) we conclude that the generation functions $\mathcal{C}_\nu(z_0)$ converges only for $\nu - \mu = \theta < 1$ (recall that $\nu \geqslant \mu$). Hence Eq. (19) may not be satisfied to cancel the terms corresponding to the factor $(1 - z')^{\tau+\nu-1}$. The failure of this asymptotic analysis seemingly manifests the change of the evolution regime, which has been observed in the numerical simulations: For $\theta > 1$ the oscillations of concentrations emerge—the systems either relax to a steady state through damped oscillations, or demonstrate never-ending oscillations.

B. Qualitative analysis

To understand the mechanism of the stable oscillations let us consider a special Brownian kernel with $\nu = -\mu = a = 1$. The monomer density satisfies

$$\frac{dn_1}{dt} = \lambda(N + M_2 M_{-1}) - (1+\lambda)n_1(1 + M_{-1}) \tag{30}$$

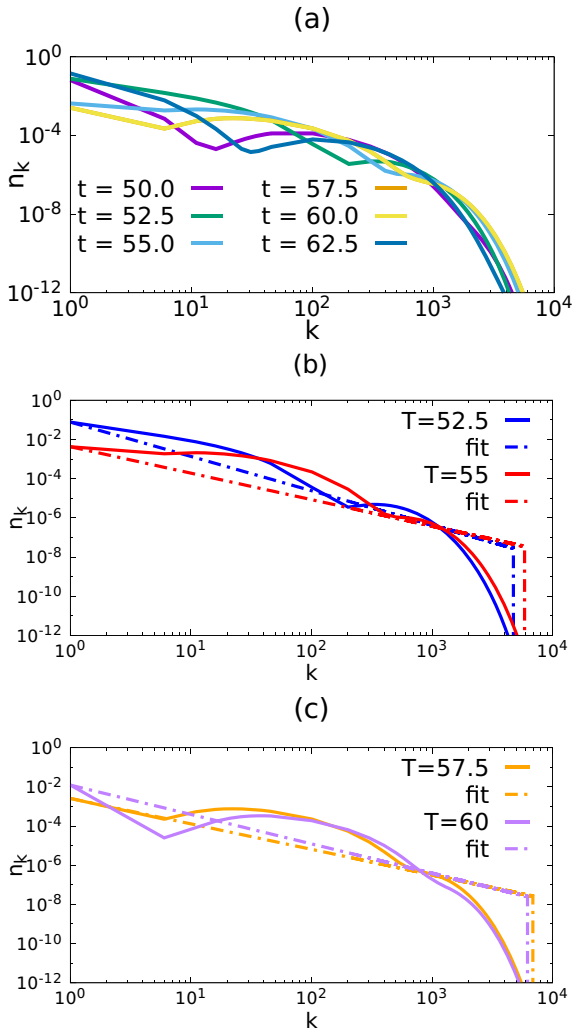

FIG. 9. Top panel: Time dependence of $n_k(t)$. The effective slope of the distribution and the effective cutoff size $k_{\max}$ periodically change with time. Middle and bottom panels: The real and coarse-grained cluster size distributions. The smooth cutoff of the real distribution is approximated by the abrupt model cutoff. The simulation data are shown for the kernel (7) with $a = 0.95$ and $\lambda = 0.005$.

and the rate equation for the cluster density is

$$\frac{dN}{dt} = \lambda(N + M_2 M_{-1}) - (1 + 2\lambda)M_{-1}. \tag{31}$$

(We set $M = 1$.) These equations are not closed as they involve the moments M_{-1} and M_2. One can write the rate equation for M_2, but it involves the third moment M_3. This continues *ad infinitum* leading to an analytically unsolvable hierarchy.

Note that on the right-hand side of Eq. (30) one term is negative and the other one is positive; the first is of the order of n_1 and the second is of the order λM_2. Initially only small clusters are present in the system, so that λM_2 is small for $\lambda \ll 1$ and n_1 decreases. Due to the conservation of mass the decrease of n_1 implies the increase of other concentrations. Hence, after some time a wider cluster size distribution is established, such that λM_2 increases. When it exceeds n_1, the right-hand side of Eq. (30) becomes positive and n_1 starts to grow. Due to the conservation of mass, the growth of n_1 implies the decay of other concentrations, which leads to the decrease of M_2 and eventually to the negative sign of the right-hand side of Eq. (30). Then the cycle repeats.

Let us try to put the above narrative picture into somewhat more quantitative terms. First, we notice that the oscillations of concentrations correspond to the periodically varying distribution of cluster sizes, as illustrated in Fig. 9. Roughly speaking, the size distribution $n_k(t)$ behaves in such a way that the effective slope of this distribution $\alpha(t)$ and the effective cutoff $k_{\max}(t)$ periodically change in time. Averaging over these oscillations we obtain the distribution $\langle n_k \rangle_{\rm osc}$ depicted in Fig. 6.

To understand the nature of the observed behavior of the system, we develop a qualitative theory. To this end we approximate the real distribution $n_k(t)$ by a model distribution $n_k^{\rm mod}(t)$ which reflects the most prominent features of the real distribution. Namely we assume that $n_k(t)$ may be characterized by a power-law distribution with a varying slope $\alpha(t)$ and a large-size cutoff $k_{\max}(t)$; it should obey the mass conservation. Namely, we assume the following model distribution:

$$n_k^{\rm mod}(t) = \begin{cases} \frac{n_1(t)}{k^{\alpha(t)}} & \text{for } k \leqslant k_{\max}(t) \\ 0 & \text{for } k > k_{\max}(t) \end{cases}. \tag{32}$$

The real distribution of the aggregate sizes $n_k(t)$ may be approximated by the model distribution (32) applying a coarse graining. For the qualitative analysis addressed here we exploited the simplest approach. Namely, we use the value of $n_1(t)$, obtained in the simulations, and find the parameters $\alpha(t)$ and $k_{\max}(t)$ from the conservation of mass. That is, we numerically find the pair (α, $k_{\max}$) with integer $k_{\max}$, that minimizes the difference, $|n_1 H_{k_{\max},\alpha} - 1|$, where $H_{k_{\max},\alpha} = \sum_{i=1}^{k_{\max}} i^{-\alpha}$ are the generalized harmonic numbers. The variation with time of the model distribution (32), which mimics the real distribution, is shown in Fig. 9. In Fig. 10 we show the periodic variation on the model parameters $\alpha(t)$ and $n_1(t)$ and demonstrate that the variation of the slope is limited by the interval $1 < \alpha(t) < 2$.

To perform a qualitative analysis we focus on the qualitative dependence of the moments M_{-1}, N, M, and M_2 on n_1, α, and $k_{\max}$ and approximate the summation by integration:

$$M_i = \sum_{k=1}^{k_{\max}} k^i n_k \simeq b_i \int_1^{k_{\max}} k^i n_k dk, \tag{33}$$

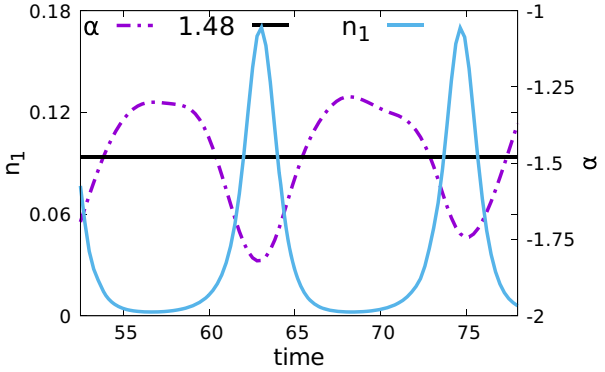

FIG. 10. Periodic variation of the model parameters $\alpha(t)$ and $n_1(t)$ for $a = 0.95$ and $\lambda = 0.005$. Only two periods of oscillations are shown. The simulation data are the same as for Fig. 9.

where we introduce the coefficients b_i. These coefficients (assumed to be constant), are of the order of 1 and account for the difference between integration and summation. Hence we obtain

$$M_{-1}(t) \simeq b_{-1}\frac{n_1(t)}{\alpha(t)}, \quad N(t) \simeq b_0\frac{n_1(t)}{\alpha(t)-1}, \\ M_2(t) \simeq b_2\frac{n_1(t)}{3-\alpha(t)}[k_{\max}(t)]^{3-\alpha(t)}, \tag{34}$$

where we use the condition $k_{\max} \gg 1$. Similarly, the conservation of mass yields the relation between $n_1(t)$, $\alpha(t)$, and $k_{\max}(t)$:

$$M = \sum_{k=1}^{k_{\max}} k n_k \simeq b_1 n_1 k_{\max}^{2-\alpha}(2-\alpha)^{-1} = 1. \tag{35}$$

Using (34) and (35), we recast (30) and (31) into

$$\dot{n}_1 = \lambda n_1\left[\frac{b_0}{\alpha-1} + \frac{b_2 b_{-1} n_1}{(3-\alpha)\alpha}\left(\frac{2-\alpha}{b_1 n_1}\right)^{(3-\alpha)/(2-\alpha)}\right] \\ -(1+\lambda)n_1\left(1+\frac{b_{-1}n_1}{\alpha}\right), \tag{36a}$$

$$\dot{\alpha} = \lambda(b_0+1-\alpha)\left[1+\frac{b_2 b_{-1}(\alpha-1)n_1}{b_0(3-\alpha)\alpha} \times\left(\frac{2-\alpha}{b_1 n_1}\right)^{(3-\alpha)/(2-\alpha)}\right] + \frac{(\alpha-1)^2(1+\lambda)}{\alpha} \\ \times\left[\frac{(1+2\lambda)b_{-1}}{(1+\lambda)b_0} - \frac{\alpha+b_{-1}n_1}{\alpha-1}\right]. \tag{36b}$$

To show that never-ending oscillations are possible we perform the linear stability analysis of Eqs. (36a) and (36b). We consider the coefficients b_i ($i = -1, 0, 1, 2$) as known and of the order of unity. Further, we assume that there is a fixed point, $n_1 = n_1^{(0)}$ and $\alpha = \alpha_0$. At the fixed point $G_1(n_1^{(0)},\alpha_0) = G_2(n_1^{(0)},\alpha_0) = 0$ where $G_1(n_1,\alpha)$ and for $G_2(n_1,\alpha)$ denote the right-hand sides of (36a) and (36b), respectively. We also shortly write

$$g_{1n} = \left.\frac{\partial G_1}{\partial n_1}\right|_{n_1^{(0)},\alpha_0}, \quad g_{1\alpha} = \left.\frac{\partial G_1}{\partial \alpha}\right|_{n_1^{(0)},\alpha_0}, \\ g_{2n} = \left.\frac{\partial G_2}{\partial n_1}\right|_{n_1^{(0)},\alpha_0}, \quad g_{2\alpha} = \left.\frac{\partial G_2}{\partial \alpha}\right|_{n_1^{(0)},\alpha_0} \tag{37}$$

and deduce the linearized equations

$$\frac{d}{dt}\begin{pmatrix}\delta n_1\\ \delta\alpha\end{pmatrix} = \begin{pmatrix} g_{1n} & g_{1\alpha}\\ g_{2n} & g_{2\alpha}\end{pmatrix}\begin{pmatrix}\delta n_1\\ \delta\alpha\end{pmatrix} \tag{38}$$

for the deviations $\delta n_1 = n_1 - n_1^{(0)}$ and $\delta\alpha = \alpha - \alpha_0$. The eigenvalues of the matrix in (38) are

$$\nu_{1,2} = \tfrac{1}{2}[g_{1n} + g_{2\alpha} \pm \sqrt{(g_{1n}-g_{2\alpha})^2 + 4g_{1\alpha}g_{2n}}]. \tag{39}$$

Oscillations may occur if the above eigenvalues possess an imaginary part. This condition, $\mathrm{Im}(\nu_{1/2}) \neq 0$, requires the negatives determinant in

$$D = (g_{1n} - g_{2\alpha})^2 + 4g_{1\alpha}g_{2n} < 0. \tag{40}$$

If the real part of the eigenvalues is negative, that is $(g_{1n} + g_{2\alpha})/2 < 0$, the fixed point is stable; in this case the cluster distribution relaxes to the steady state n_k. In the opposite case of the positive real part, $(g_{1n} + g_{2\alpha})/2 > 0$, the fixed point is linearly unstable and the oscillations grow and are eventually stabilized by nonlinear terms.

The coefficients b_i are unknown, so we cannot locate the fixed point $(n_1^{(0)},\alpha_0)$. Numerically we observe that the coefficients b_i are of the order of 1; the location of the fixed point corresponds to $n_1^{(0)} = O(\lambda)$ with α_0 in the interval $1 < \alpha_0 < 1.5$. Variation of $\{b_i\}$ leads to the variation of $n_1^{(0)}$ and α_0. Hence to simplify the qualitative analysis we directly vary $n_1^{(0)}$ and α_0, keeping $\{b_i\}$ fixed; we analyze the sign of D and $g_{1n} + g_{2\alpha}$ in the according domain, $0.1\lambda \leqslant n_1^{(0)} \leqslant 10\lambda$ and $1 < \alpha_0 < 1.5$ for different λ. The results are shown in Fig. 11.

Figure 11 demonstrates that for $\lambda = 0.0001$ there is a large area in the domain of the $(\alpha_0,n_1^{(0)})$ plane where steady oscillations may be observed. These may be either linearly stable oscillations or the growing ones, stabilized by nonlinear terms. For relatively large $\lambda = 0.1$, the steady oscillations may arise only in a tiny part of the $(\alpha_0,n_1^{(0)})$ plane. This corresponds to the kinetic regimes observed for the full set of aggregation-fragmentation equations: the emergence of the oscillations for small values of λ and their absence for large λ.

We also note that the average slope of the concentration distribution, α_0, is located within the interval $1.05 \leqslant \alpha_0 \leqslant 1.45$, see Fig. 11, with the median of 1.25. This is consistent with the slope of the averaged over oscillations distribution $\langle n_k\rangle_{\mathrm{osc}}$ depicted in Fig. 6.

C. Concentration oscillations in thermodynamically closed systems

As noted above, the time-independent rates K_{ij} and $F_{ij} = \lambda K_{ij}$ imply a steady supply of energy. This follows generally from the second law of thermodynamics, which excludes steady cyclic processes without energy supply and may be illustrated for a particular microscopic mechanism of a ballistic aggregation and shattering; this happens in planetary rings or atmospheric processes. Indeed, the conservation of momentum of coalescing particles dictates a withdrawal of a part of their kinetic energy, associated with the relative motion. This energy is transmitted either to the internal degrees of freedom of the particles (as in planetary rings), or to the surrounding gas (as in atmospheric processes). Similarly, the total kinetic energy of fragments is smaller than the initial kinetic energy of the colliding aggregates, since part of the energy is spent to break interfragment bonds. Hence, both aggregation and fragmentation processes lead to a gradual reduction of the total kinetic energy of the system. This causes a slowdown of both processes, and the respective decrease of the rate coefficients. Here we consider thermodynamically closed systems, where the energy supply is lacking. Namely, we consider systems of particles that suffer ballistic aggregation and fragmentation. We chose such systems since the corresponding microscopic rates K_{ij} and F_{ij} are available [10,13,16]; see the Appendix.

Physically, the decay of kinetic energy causes a permanent decrease of collision frequency and the according decrease of the kinetic rates. Moreover, the fragmentation rates

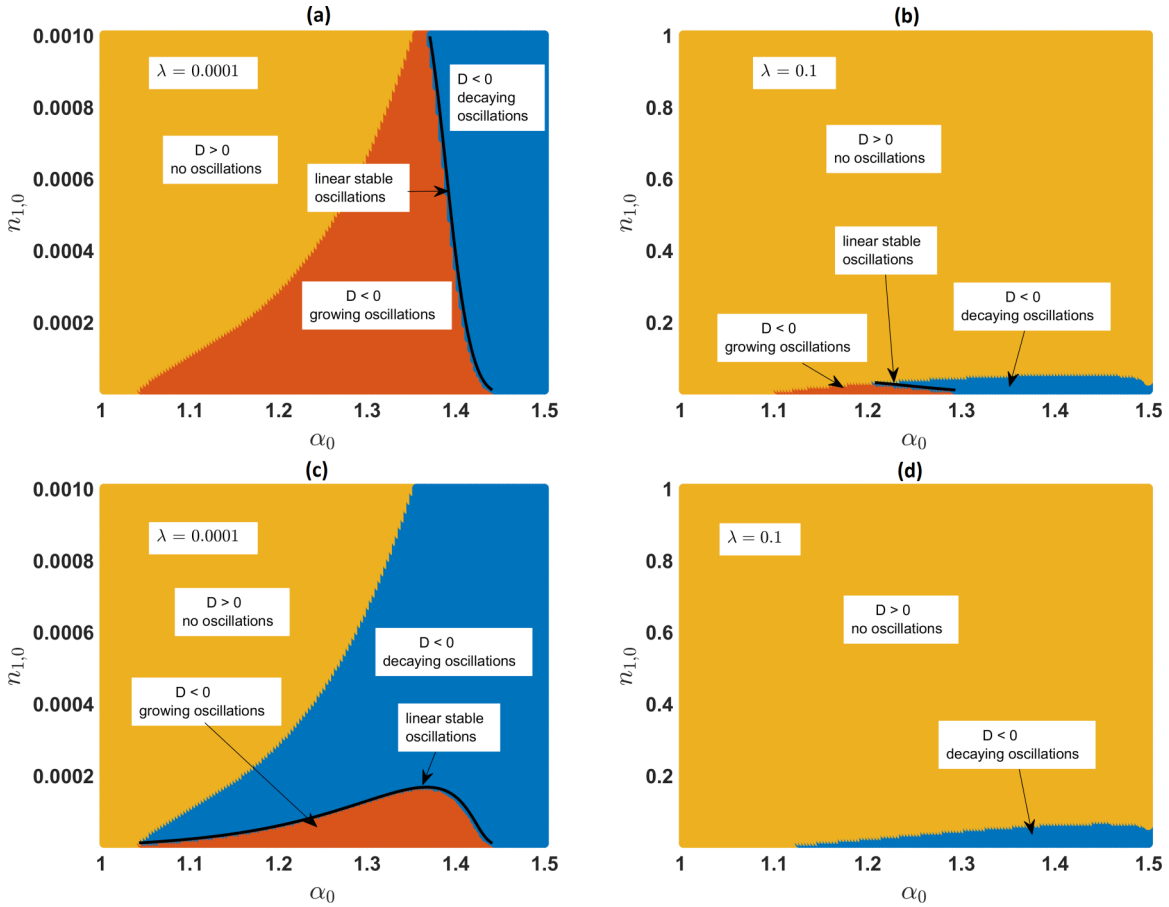

FIG. 11. Kinetic regimes for different location of the fixed point, $(\alpha_0, n_1^{(0)})$, as it follows from Eqs. (39) and (40) for $\lambda = 0.0001$ (left panels) and $\lambda = 0.1$ (right panels) and the coefficients $b_{-1} = 2$, $b_0 = 0.5$, $b_1 = 1$, $b_2 = 1$ (a),(b) and $b_{-1} = 0.25$, $b_0 = 0.5$, $b_1 = 1$, $b_2 = 1$ (c),(d). For the negative determinant ($D < 0$) the oscillations emerge. The stability of the oscillations is determined by the sign of $g_{1n} + g_{2\alpha}$. Note that for large $\lambda = 0.1$ (right panels) stable oscillation, both linearly stable and linearly unstable (with the nonlinear stabilization), may arise in a very small area of the parametric space, while for small $\lambda = 0.0001$ (left panels) the according domain is rather large.

additionally decrease, since the fraction of fast particles, which cause shattering, also drops down. Referring for detail to the Appendix, we present here the equations for aggregation and shattering for thermodynamically closed systems:

$$\frac{dn_1}{dt} = -n_1 \sum_{i=1}^{\infty} K_{1,i} n_i + \frac{\lambda}{2} \sum_{i=2}^{\infty} \sum_{j=2}^{\infty} (i+j) K_{i,j} n_i n_j + \lambda n_1 \sum_{j=2}^{\infty} j K_{1,j} n_j, \tag{41}$$

$$\frac{dn_k}{dt} = \frac{1}{2} \sum_{i=1}^{k-1} K_{i,k-i} n_i n_{k-i} - (1+\lambda) n_k \sum_{i=1}^{\infty} K_{k,i} n_i \tag{42}$$

$$\lambda = \exp[-A(1+Bt)^b]. \tag{43}$$

K_{ij} in the above Eqs. (41) and (42), are defined by Eq. (5). Time is measured in collision units, $\tau_c^{-1} = 2\sqrt{2\pi}\sigma^2 n_{1,0}\sqrt{T(t)/m}$, where σ, m, and $n_{1,0}$ are respectively the diameter, mass, and initial concentration of monomers and $T(t)$ is the characteristic temperature. The concentration of aggregates is measured in units of the initial concentration of monomers, $n_{1,0}$. The constants A, B, and b in Eq. (43) are expressed respectively in terms of the characteristic fragmentation energy and temperature decay rate (see the Appendix for the detail). Note that while λ is constant in Eqs. (3) and (4), it decays with time in Eqs. (41) and (42).

The results of numerical solution of Eqs. (41)–(43) is presented in Fig. 12. As may be seen from the figure the persistent concentration oscillations emerge in thermodynamically closed systems. Since the time for the depicted oscillations is measured in the collision units, one concludes that the period of these oscillations steadily increases with time; this is also visible in the collision time scale. As one can see from Fig. 12, in thermodynamically closed systems there exists a regime when the oscillations first decay and then again grow.

IV. CONCLUSIONS

We have studied numerically and analytically a class of aggregation-fragmentation models with a conservation of mass, which lack source and sinks of particles. It is described by the infinite set of Smoluchowski-like equations with the homogeneous aggregation and fragmentation kernels which respectively read $K_{i,j} = i^\nu j^\mu + j^\nu i^\mu$ and $F_{i,j} = \lambda K_{i,j}$, where the parameter λ quantifies the intensity of fragmentation. We consider the case of a complete decomposition (shattering) of colliding aggregates into monomers. This model and a similar

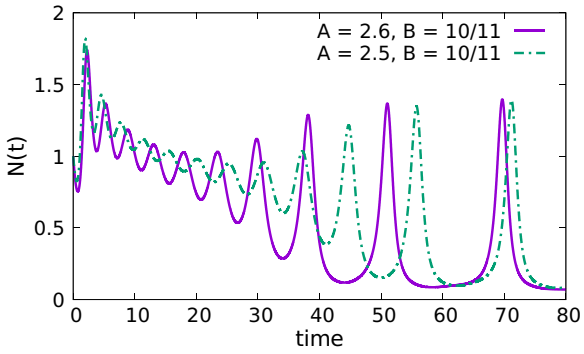

FIG. 12. Concentration oscillation in thermodynamically closed systems with aggregation and shattering. Time is measured in collision units, which keeps the aggregation rates $K_{i,j} = (i/j)^a + (j/i)^a$ with $a = 0.98$, steady, but corresponds to slowing down in the laboratory time. The shattering coefficient $\lambda = \lambda(t) = e^{-A(1+Bt)^{0.2}}$ decreases with time according to Eq. (43) with $b = 0.2$ and different coefficients A and B. The persistent oscillations are clearly visible.

model, with a source of monomers and evaporation (instead of shattering) of large clusters has been studied recently in [17,18]. For the kernels with $\theta = \nu - \mu < 1$ we obtain an analytical solution for the steady-state size distribution of the aggregates n_k and confirm numerically the relaxation of the size distribution to this steady-state form. For kernels with $\theta = \nu - \mu > 1$, we observe that the dynamic of the system dramatically depends on the value of the fragmentation constant λ. While for $\lambda < \lambda_c$ the system relaxes to a steady state through damped oscillations of concentrations, for $\lambda \geqslant \lambda_c$ no steady-state distribution of the cluster size has been detected.

The emergence of stable oscillations in a closed system of aggregating and fragmenting particles, that lacks any sinks and sources of mass, and formally corresponds to an infinite number of species, is surprising. Persistent oscillations have been detected not only for systems closed with respect to the total mass, but also for *thermodynamically* closed systems, when the notion "thermodynamics" is meaningful. In Ref. [27] stable oscillations have been detected numerically for Smoluchowski equations for an open system of reversibly aggregating particles (without fragmentation) with a source of monomers and sink of large clusters, which makes the system finite. For a small closed system comprising monomer, dimers, trimers, and exited monomers, stable oscillations of concentrations have been also reported [28]. Similarly, steady chemical oscillations have been found in a simple dimerization model (see, e.g., [29] and references therein).

Our findings may help one to understand various phenomena observed in the systems with aggregation and fragmentation, in particular the periodic formation and destruction of clumps in F Ring of Saturn [41], where particles of different mass suffer aggregative and disruptive impacts, presumably under the mass conservation condition. A complete understanding of this phenomenon is presently lacking.

ACKNOWLEDGMENT

This work has been partly supported by the Russian Science Foundation, Grant No. 14-11-00806.

APPENDIX

General expressions for the aggregation and fragmentation rates for a system of ballistically moving particles (molecules, macroscopic grains, etc.) that suffer pairwise collisions have been reported in Refs. [10,13]. These read in the present notations

$$\begin{aligned} K_{ij} &= \nu_{ij}[1 - (1 + B_{ij}\tilde{E}_{\rm agg})e^{-B_{ij}\tilde{E}_{\rm agg}}], \\ F_{ij} &= \nu_{ij}e^{-B_{ij}E_{\rm frag}}, \\ \nu_{ij} &= 2\sqrt{2\pi}\sigma_{ij}^2\sqrt{\frac{T_i}{m_i} + \frac{T_j}{m_j}}, \\ B_{ij} &= \frac{m_i^{-1} + m_j^{-1}}{T_i/m_i + T_j/m_j}, \end{aligned} \tag{A1}$$

where T_i are partial temperatures of aggregates of size i, and mass $m_i = m_1 i$ (m_1 is the mass of monomer), that characterizes the average kinetic energy of such aggregates [10,13,16]. $E_{\rm agg}$ and $E_{\rm frag}$ are respectively the aggregation and fragmentation energy, $\tilde{E}_{\rm agg} = E_{\rm agg}/\varepsilon^2$, where ε is the coefficient of normal restitution that characterizes dissipative losses in the impacts [16]. $\sigma_{ij} = \sigma_1(i^{1/D} + j^{1/D})$, where σ_1 is monomer diameter and D is the dimension of the aggregates, which may be fractal. Based on the results of Ref. [42], we assume that partial temperatures scale as $T_i(t) = T(t)i^\gamma$, where $T(t)$ is the characteristic temperature of the gas mixture. (It may be shown that after a short relaxation time the rate of change of temperatures of all species is the same, $T_i^{-1}dT_i/dt = T^{-1}dT/dt$ [42].)

It is convenient to recast the above kinetic coefficients into the form

$$\begin{aligned} K_{ij} &= \tau_0^{-1}(T/T_0)^{1/2}n_{1,0}^{-1}\tilde{K}_{ij}, \\ \tilde{K}_{ij} &= (i^{1/D} + j^{1/D})^2(i^{\gamma-1} + j^{\gamma-1})^{1/2}, \\ F_{ij} &= \lambda K_{ij} \qquad \lambda \approx \exp\left[-A\,(T_0/T)\right], \end{aligned} \tag{A2}$$

where $n_{1,0}$ is the initial concentration of monomers, which we will use as a unit of concentration, T_0 is the initial characteristic temperature, and

$$\tau_0^{-1} = 2\sqrt{2\pi}\sigma_0^2 n_{1,0}(T_0/m_1)^{1/2} \tag{A3}$$

gives the initial characteristic collision frequency. The quantity A is the effective average ratio of fragmentation and kinetic energy, $A = (E_{\rm frag}/T_0)\langle(i^{-1} + j^{-1})/(i^{\gamma-1} + j^{\gamma-1})\rangle$. We also assume for simplicity that the aggregation energy is large, so that $B_{ij}\tilde{E}_{\rm agg} \gg 1$.

The dimensionless kernels $\tilde{K}_{ij}$ are obtained by a straightforward solution of the Boltzmann equation [10,13,16]. Here we apply a standard simplification [1,2] for these kernels, which allows analytical analysis. It is based on the observation that the main properties of the solutions to the Smoluchowski equations depend on two indices β and β_1, characterizing the kinetic rates K_{ij}. The first index quantifies the homogeneity degree of a kernel, and the second one the size dependence at the maximal size asymmetry. Namely,

$$\tilde{K}_{ai,aj} \sim a^\beta \tilde{K}_{ij}; \quad \tilde{K}_{1,j} \sim j^{\beta_1} \quad \text{for} \quad i, j \gg 1.$$

For the kernels

$$\tilde{K}_{ij} = i^{\nu} j^{\mu} + i^{\mu} j^{\nu}$$

introduced in Eq. (5), one has $\beta = \nu + \mu$ and $\beta_1 = \max(\nu,\mu)$. Hence, Eqs. (A2) show that the indices ν and μ are related to the physical parameters D and γ as $(\nu,\mu) = (2/D,(\gamma-1)/2)$ for $\gamma < 1$ and $(\nu,\mu) = (2/D + (\gamma-1)/2,0)$ for $\gamma > 1$.

Next, we derive the equation for the characteristic temperature $T(t)$. This may be done using the approach of Ref. [16], which yields

$$\frac{d}{dt} NT = -\sum_{ij} Q_{ij}(T) n_i n_j + \sum_i \Gamma_i n_i. \tag{A4}$$

Here $Q_{ij}(T)$ are temperature-dependent rate coefficients and Γ_i describes the energy input to the system due to the interaction of the aggregates of size i with the external sources of energy (see also [42]). Here we do not need explicit expressions for these quantities. We just state that the presence of the energy sources Γ_i in Eq. (A4) yields the solutions with a constant temperature $T = \text{const.}$, corresponding to the systems with time-independent rates K_{ij} and F_{ij}. For thermodynamically closed systems, the temperature commonly decreases with time (see the discussion in Ref. [16]).

The solutions of the coupled Smoluchowski-like equations (A2) and (A4) for concentrations and temperature is beyond the scope of the present study. For the qualitative analysis, we assume a power-law decay of the characteristic temperature with time, $T = T_0(1 + t/\tau_0)^{-\delta}$; such assumption is justified by the results of Ref. [16]. The value of δ depends on the parameters of the system and may vary in a wide interval [16]. Using the collision frequency, $\tau_c^{-1}(t) = \tau_0^{-1}[T(t)/T_0]^{1/2}$ at the current time t, we introduce a new dimensionless time $\tilde{t}$, measured in collision units. It is related to the laboratory time as $\tau_c^{-1}(t)dt = d\tilde{t}$. The dependence of temperature on the new time then reads

$$T/T_0 = [1 + B\tilde{t}\,]^{-b}, \tag{A5}$$

where $b = 2\delta/(2-\delta)$ and B is a constant. The kinetic rates may be also expressed in terms of the collision-based time $\tilde{t}$:

$$K_{ij} = \tau_c^{-1}(\tilde{t}\,) n_{1,0}^{-1} \tilde{K}_{ij}, \tag{A6}$$

$$\lambda = \exp[-A(1 + B\tilde{t}\,)^b]. \tag{A7}$$

In our simulations we choose $b = 0.2$ (which corresponds to $\delta = 2/11$).

Substituting the rates K_{ij} and coefficient λ from Eqs. (A6) and (A7) into Eqs. (3) and (4), we arrive at Eqs. (41)–(43), where time is measured in the collision units and concentrations in the units of initial concentration of monomers. For simplicity we use in these equations the same notations as in Eqs. (3) and (4).

[1] P. L. Krapivsky, S. Redner, and E. Ben-Naim, *A Kinetic View of Statistical Physics* (Cambridge University Press, Cambridge, England, 2010).
[2] F. Leyvraz, Phys. Rep. **383**, 95 (2003).
[3] T. Poeschel, N. V. Brilliantov, and C. Frommel, Biophys. J. **85**, 3460 (2003).
[4] R. C. Shrivastava, J. Atmos. Sci. **39**, 1317 (1982).
[5] S. B. Grant, Environ. Sci. Technol. **28**, 928 (1994).
[6] H. Niwa, J. Theor. Biol. **195**, 351 (1998).
[7] W. Miura, H. Takayasu, and M. Takayasu, Phys. Rev. Lett **108**, 168701 (2012).
[8] S. N. Dorogovtsev and J. F. F. Mendes, *Evolution of Networks: From Biological Nets to the Internet and WWW* (Oxford University Press, New York, 2003).
[9] V. E. Zakharov, V. S. L'vov, and G. Falkovich, *Kolmogorov Spectra of Turbulence I: Wave Turbulence* (Springer, New York, 2012).
[10] N. V. Brilliantov, P. L. Krapivsky, A. Bodrova, F. Spahn, H. Hayakawa, V. Stadnichuk, and J. Schmidt, Proc. Natl. Acad. Sci. USA **112**, 9536 (2015).
[11] V. Stadnichuk, A. Bodrova, and N. V. Brilliantov, Int. J. Mod. Phys. B **29**, 1550208 (2015).
[12] J. N. Cuzzi, J. A. Burns, S. Charnoz, R. N. Clark, J. E. Colwell, L. Dones, L. W. Esposito, G. Filacchione, R. G. French, M. M. Hedman *et al.*, Science **327**, 1470 (2010).
[13] N. V. Brilliantov, A. S. Bodrova, and P. L. Krapivsky, J. Stat. Mech. (2009) P06011.
[14] L. Esposito, *Planetary Rings* (Cambridge University Press, Cambridge, England, 2006).
[15] P. L. Krapivsky, W. Otieno, and N. V. Brilliantov, Phys. Rev. E **96**, 042138 (2017).
[16] N. Brilliantov, A. Formella, and T. Poeschel, Nat. Commun. **9**, 797 (2018).
[17] C. Connaughton, A. Dutta, R. Rajesh, and O. Zaboronski, Europhys. Lett. **117**, 10002 (2017).
[18] C. Connaughton, A. Dutta, R. Rajesh, N. Siddharth, and O. Zaboronski, Phys. Rev. E **97**, 022137 (2018).
[19] E. M. Hendriks, M. H. Ernst, and R. M. Ziff, J. Stat. Phys. **31**, 519 (1983).
[20] P. G. J. van Dongen, J. Phys. A **20**, 1889 (1987).
[21] N. V. Brilliantov and P. L. Krapivsky, J. Phys. A **24**, 4789 (1991).
[22] P. Laurençot, Nonlinearity **12**, 229 (1999).
[23] L. Malyushkin and J. Goodman, Icarus **150**, 314 (2001).
[24] P. L. Krapivsky and C. Connaughton, J. Chem. Phys. **136**, 204901 (2012).
[25] R. C. Ball, C. Connaughton, T. H. M. Stein, and O. Zaboronski, Phys. Rev. E **84**, 011111 (2011).
[26] H. Hayakawa, J. Phys. A **20**, L801 (1987).
[27] R. C. Ball, C. Connaughton, P. P. Jones, R. Rajesh, and O. Zaboronski, Phys. Rev. Lett. **109**, 168304 (2012).
[28] V. I. Bykov and A. N. Gorban, Chem. Eng. Sci. **42**, 1249 (1987).
[29] M. Stich, C. Blanco, and D. Hochberg, Phys. Chem. Chem. Phys. **15**, 255 (2013).
[30] S. A. Matveev, P. L. Krapivsky, A. P. Smirnov, E. E. Tyrtyshnikov, and N. V. Brilliantov, Phys. Rev. Lett. **119**, 260601 (2017).
[31] D. Helbing, Rev. Mod. Phys. **73**, 1067 (2001).

[32] S. K. Friedlander, *Smoke, Dust and Haze*, 2nd Edition (Oxford University Press, Oxford, 2000).
[33] V. Ossenkopf, Astron. Astrophys. **280**, 617 (1993).
[34] N. V. Brilliantov and F. Spahn, Math. Comput. Simul. **72**, 93 (2006).
[35] S. A. Matveev, A. P. Smirnov, and E. E. Tyrtyshnikov, J. Comput. Phys. **282**, 23 (2015).
[36] A. Chaudhury, I. Oseledets, and R. Ramachandran, Comput. Chem. Eng. **61**, 234 (2014).
[37] W. Hackbusch, Computing **78**, 145 (2006).
[38] W. Hackbusch, Numer. Math. **106**, 627 (2007).
[39] S. Matveev, N. Ampilogova, V. Stadnichuk, E. E. Tyrtyshnikov, A. Smirnov, and N. Brilliantov, Comput. Phys. Commun. **224**, 154 (2018).
[40] S. H. Strogatz, *Nonlinear Dynamics and Chaos* (Addison-Wesley, New York, 1994).
[41] R. S. French, S. K. Hicks, M. R. Showalter, A. K. Antonsen, and D. R. Packard, Icarus **241**, 200 (2014).
[42] A. Bodrova, D. Levchenko, and N. V. Brilliantov, Europhys. Lett. **106**, 14001 (2014).